

# The effect of fuel feeding method on performance of SOFC–PEFC system

M. Yokoo<sup>a,\*</sup>, K. Watanabe<sup>a</sup>, M. Arakawa<sup>a</sup>, Y. Yamazaki<sup>b</sup>

<sup>a</sup> *NTT Energy and Environment Systems Laboratories, NTT Corporation, 3-1, Morinosato, Wakamiya, Atsugi-shi, Kanagawa 243-0198, Japan*

<sup>b</sup> *Department of Innovative and Engineered Materials, Interdisciplinary Graduate School of Science and Engineering, Tokyo Institute of Technology, 4259, Nagatsuta, Midoriku, Yokohama-shi, Kanagawa 226-8502, Japan*

Received 30 September 2005; received in revised form 28 November 2005; accepted 30 November 2005

Available online 10 January 2006

## Abstract

We evaluate two kinds of solid-oxide-fuel-cell (SOFC)–polymer-electrolyte-fuel-cell (PEFC) combined systems by numerical simulation to investigate the effect of the fuel feeding method. In one, fuel for the system is reformed by using exhaust heat from the SOFC and is separately supplied to the SOFC and PEFC (parallel SOFC–PEFC system). In the other, fuel is fed to the SOFC first and then SOFC exhaust fuel is fed to the PEFC (series SOFC–PEFC system). The quality of the fuel gas in the SOFC is better in the latter system, whereas the quality of the fuel gas in the PEFC is better in the former. We demonstrate that larger PEFC output can be obtained in the parallel SOFC–PEFC system, since more steam, which is included in the SOFC anode exhaust gas, can be used for the reforming of the fuel for the PEFC. We show that the series SOFC–PEFC system provides higher electrical efficiency because the fuel gas quality has a stronger influence on the electromotive force in the SOFC than in the PEFC.

© 2005 Elsevier B.V. All rights reserved.

**Keywords:** Solid oxide fuel cell; Polymer electrolyte fuel cell; Combined system; Steam reforming

## 1. Introduction

Power generating systems using solid oxide fuel cells (SOFCs) provide higher electrical efficiency than systems using other fuel cell because high-temperature SOFC exhaust heat ( $\approx 1073$  K) is used for fuel reforming [1]. A system using SOFCs only (simple SOFC system) has achieved 46% electrical efficiency at 109 kW ac [2]. However, that power generation systems in which an SOFC is used in combination with other generating equipment can provide higher electrical efficiency than the simple SOFC system [1]. This is because the high-temperature SOFC exhaust heat contributes to power generation in the other generating equipment.

Although systems combining an SOFC and gas turbine (SOFC–GT systems) are attracting attention [3,4], we focus on systems combining an SOFC with a polymer electrolyte fuel cell

(PEFC) [5,6]. This is because the SOFC–PEFC system is quieter than SOFC–GT systems and because the cost of the auxiliary equipment is lower [5]. In addition, SOFC–PEFC systems can provide higher efficiency than SOFC–GT systems when the output is relatively small, because the efficiency of the PEFC stack remains almost constant even as the output decreases [5,6].

Various SOFC–PEFC system configurations are possible [5–8]. We classify SOFC–PEFC systems into two types depending on the fuel feeding method. In one type, fuel for the system is reformed using exhaust heat from the SOFC and is separately supplied to the SOFC and PEFC. We refer this type of SOFC–PEFC system as a parallel SOFC–PEFC system. In the other type, all fuel is fed to the SOFC stack first and then SOFC exhaust fuel is fed to the PEFC stack. We call this type of SOFC–PEFC system a series SOFC–PEFC system. The basic concept of both systems is the same. That is, higher electrical efficiency is achieved in the SOFC–PEFC system than in the simple SOFC system by using the SOFC exhaust heat for the reforming of fuel for both the SOFC and PEFC. However, temperature and gas component profiles in the cells, which influence

\* Corresponding author. Tel.: +81 46 240 2572; fax: +81 46 270 2702.  
E-mail address: [m.yokoo@aecl.ntt.co.jp](mailto:m.yokoo@aecl.ntt.co.jp) (M. Yokoo).

**Nomenclature**

<i>C</i>	constant
<i>F</i>	Faraday’s constant ( $C\ mol^{-1}$ )
$\Delta G$	Gibbs free energy change ( $J\ mol^{-1}$ )
<i>J</i>	current density ( $A\ m^{-2}$ )
<i>L</i>	length of tubular SOFC (m)
<i>m</i>	molar fraction
<i>M</i>	molar flow rate ( $mol\ s^{-1}$ )
<i>Q</i>	amount of heat (W)
<i>R</i>	gas constant ( $J\ mol^{-1}\ K^{-1}$ )
<i>U</i>	utilization (%)
<i>V</i>	cell voltage (V)
<i>W</i>	output (W)
<i>x</i>	coordinate along gas flow (m)

*Greek letters*

$\phi$	overpotential (V)
$\eta$	electrical efficiency (%)

*Subscripts*

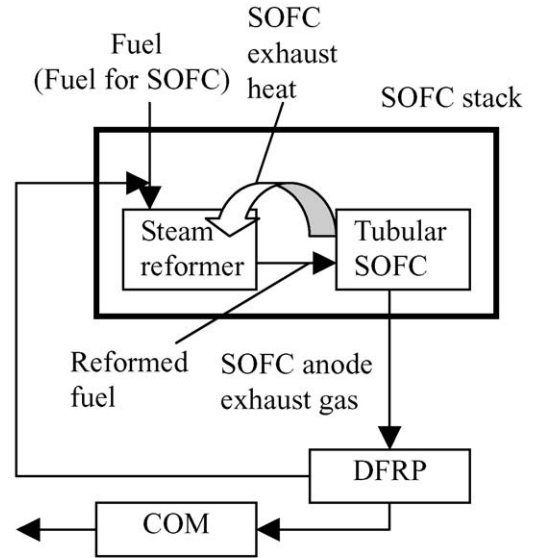
AIR	air
ANO	anode
AVE	average
CATH	cathode
FUEL	fuel
IN	inlet
OUT	outlet
PARA	parallel SOFC–PEFC system
PE	PEFC
REF	reform
SERIES	series SOFC–PEFC system
SIMP	simple SOFC system
SO	SOFC
TOT	total

cell performance, are not the same in these systems. In this study, we quantitatively evaluate these SOFC–PEFC systems and clarify the features of both.

**2. System models and the exhaust heat utilization mechanism**

**2.1. Models**

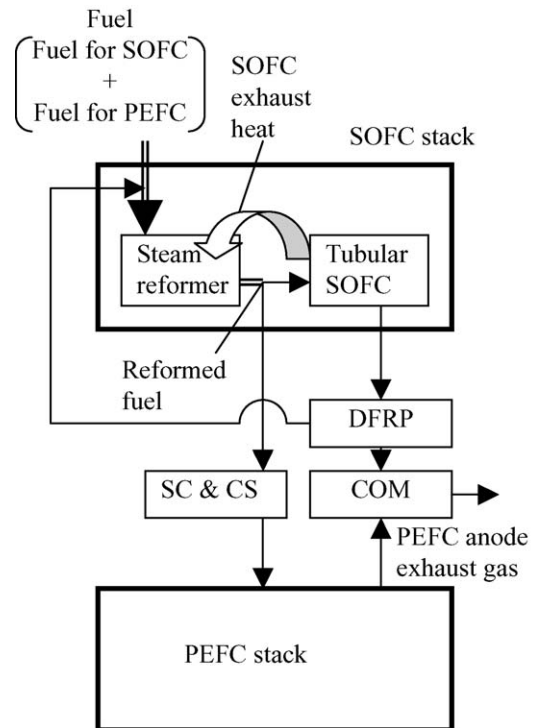
A schematic diagram of the simple SOFC system [2,5] is shown in Fig. 1. A sealless tubular SOFC stack with a depleted fuel recycling plenum and steam reformer [2–5] is used for the model of the SOFC. The steam reformer is installed adjacent to the tubular SOFCs and SOFC exhaust heat is used for the steam reforming of fuel for the SOFC. Reformed fuel is fed to the SOFC stack and used for power generation. SOFC anode exhaust gas is fed to the depleted fuel recycling plenum. Part of the SOFC anode exhaust gas is recycled to the steam reformer to feed steam. The remaining SOFC anode exhaust gas is fed to the combustor and burnt off.



COM: Combustor, DFRP: Depleted fuel recycling plenum,

Fig. 1. Simple SOFC system.

The parallel SOFC–PEFC system consists of SOFC and PEFC stacks as shown in Fig. 2. A sealless tubular SOFC stack with a depleted fuel recycling plenum and steam reformer is also used for the model of the SOFC. In this model, the fuel for



COM: Combustor, CS: CO selective oxidizer, DFRP: Depleted fuel recycling plenum, SC: Shift converter

Fig. 2. Parallel SOFC–PEFC system.

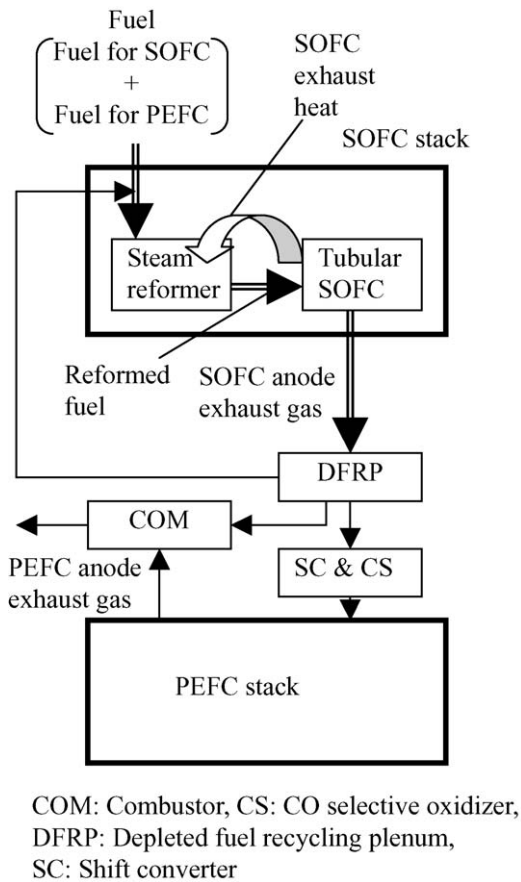


Fig. 3. Series SOFC-PEFC system.

SOFC and that for PEFC are fed to the steam reformer and they are reformed using the SOFC exhaust heat. Part of the reformed fuel is fed to the tubular SOFC and the rest is fed to the PEFC stack. Part of the SOFC anode exhaust gas is recycled to the steam reformer. The remaining SOFC anode exhaust gas and the PEFC anode exhaust gas are fed to the combustor.

Fig. 3 is a schematic diagram of the series SOFC-PEFC system. In this system, the fuel for SOFC and that for PEFC are fed to the steam reformer. As in the parallel-feed system, the SOFC exhaust heat is used for the steam reforming of fuels for both stacks. All reformed fuel is fed to the tubular SOFC first and used for power generation under the low fuel utilization condition. (In this paper, the fuel utilization of SOFC is defined as the rate of fuel used for power generation to the fuel fed to the SOFC.) Then, part of the SOFC anode exhaust gas is fed to the PEFC stack via shift converter and CO selective oxidizer. The other part of the SOFC anode exhaust gas is recycled to the steam reformer. The remaining SOFC anode exhaust gas and the PEFC anode exhaust gas are fed to the combustor.

## 2.2. Exhaust heat utilization mechanism in the SOFC-PEFC system

The SOFC exhaust heat utilization mechanism we used in the simulation is illustrated in Fig. 4, where  $Q_{REF}$  is the SOFC exhaust heat used in the steam reformer as reaction heat and  $Q_{AIR}$  is the SOFC exhaust heat discharged with air for SOFC.

## Simple SOFC system

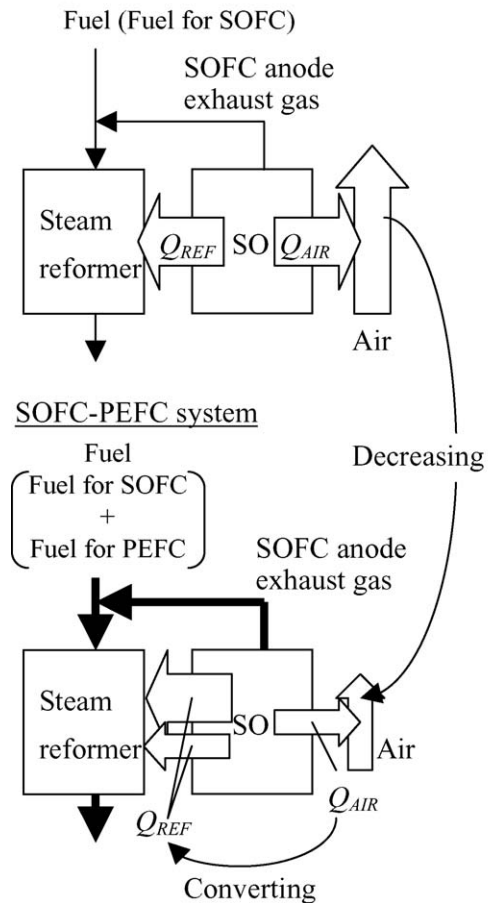
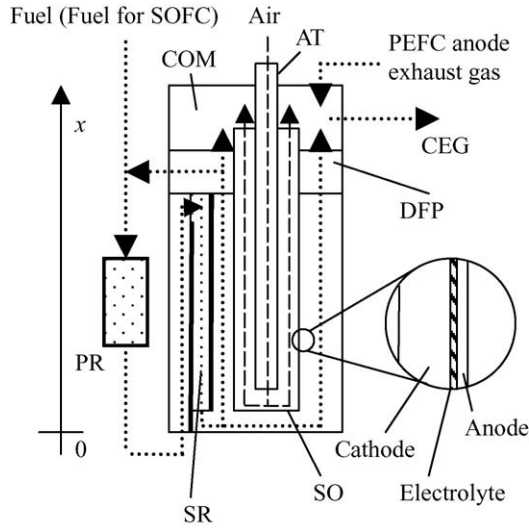


Fig. 4. SOFC exhaust heat utilization mechanism.

The point is how the SOFC exhaust heat is used for the reforming of fuels for both the SOFC and PEFC in the SOFC-PEFC systems when the SOFC operation temperature, i.e., the maximum temperature in the tubular SOFC, is kept constant at that in the simple SOFC system. Part of the SOFC exhaust heat is used for fuel reforming as  $Q_{REF}$  and part of it is discharged with the air for the SOFC as  $Q_{AIR}$ . The  $Q_{AIR}$  is almost as large as  $Q_{REF}$  in an actual 100-kW-class simple SOFC system [2]. Here,  $Q_{AIR}$  can be decreased by decreasing the air for the SOFC, since  $Q_{AIR}$  is almost proportional to the air flow rate. Therefore,  $Q_{REF}$  can be increased by converting the decrement of  $Q_{AIR}$  to  $Q_{REF}$  while the SOFC operation temperature is kept constant. That is,  $Q_{REF}$  can be increased by decreasing the air for the SOFC, while the SOFC operation temperature is kept constant. The SOFC anode exhaust gas is recycled to the steam reformer to feed the steam. Note that much more SOFC anode exhaust gas has to be recycled to the steam reformer in the SOFC-PEFC systems than in the simple SOFC system, since much more steam is needed to reform the fuel for the SOFC and PEFC.

## 3. Simulation

The simulation was performed to quantitatively compare the features of the two SOFC-PEFC systems and compare their



AT: Alumina tube, CEG: Combustion exhaust gas, COM: Combustor, DFP: Depleted fuel recycling plenum, PR: Pre-reformer, SR: Stack reformer, SO: SOFC

Fig. 5. SOFC stack unit for the simple SOFC system.

features with those of the simple SOFC system. The cell area of the SOFC stack is assumed to be same for all three systems in the simulation. The cell areas of the PEFC stacks in the SOFC–PEFC systems are varied as the simulation parameter.

### 3.1. Sealless tubular SOFC stacks

The SOFC stack for the simple SOFC system consists of 1152 SOFC stack units like the one shown in Fig. 5. The active cell area of the tubular SOFC is the same as that of the tubular SOFC in an actual simple 100-kW-class SOFC system [2], which means that the SOFC stack is 100-kW-class [2]. The total cell area of the SOFC stack is listed in Table 1. The tubular SOFCs are electrically connected to each other through Ni felt in the SOFC stack [9]. The same quantity of fuel and the same quantity of air are assumed to be supplied to each unit. All tubular SOFCs are assumed to have the same characteristics in the simulation. The fuel for the SOFC is fed to the tubular SOFC through the reformer. The steam reforming reaction of methane,



and the shift reaction,



Table 1  
Total cell areas of the SOFC and PEFC stacks

	SOFC stack (100-kW- class)	PEFC stack (25-kW- class)	PEFC stack (50-kW- class)	PEFC stack (75-kW- class)
Total cell area (m <sup>2</sup> )	96.1	19.1	38.1	57.2

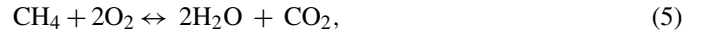
both occur in the reformer. The reaction rate of the steam reforming is determined by the equation used in our previous work [5]. The shift reaction is assumed to be in thermodynamic equilibrium in the reformer [10]. The oxidation of hydrogen,



the oxidation of carbon monoxide,



and the oxidation of methane,



are assumed to occur in the tubular SOFC as cell reactions. The partial pressure of each gas component is assumed to be in thermodynamic equilibrium at the anode side [11]. The temperature profiles of the anode, cathode, and electrolyte are assumed to be the same. The voltage drop in the tubular SOFC is assumed to be caused by ohmic resistance of the cathode and contact resistance between the tubular SOFC and Ni felt. The contact resistance between the tubular SOFC and Ni felt was estimated from the experimental results [2, 12]. Overpotential is assumed to be approximated to the ohmic resistance. The cell voltage  $V_{\text{SO}}$  is calculated so that the average current density of the SOFC stack is  $2000 \text{ A m}^{-2}$  based on the equation:

$$V_{\text{SO}} = E_{\text{SO}}(x) - \phi_{\text{SO}}(x) - J_{\text{SO}}(x)\Gamma, \quad (6)$$

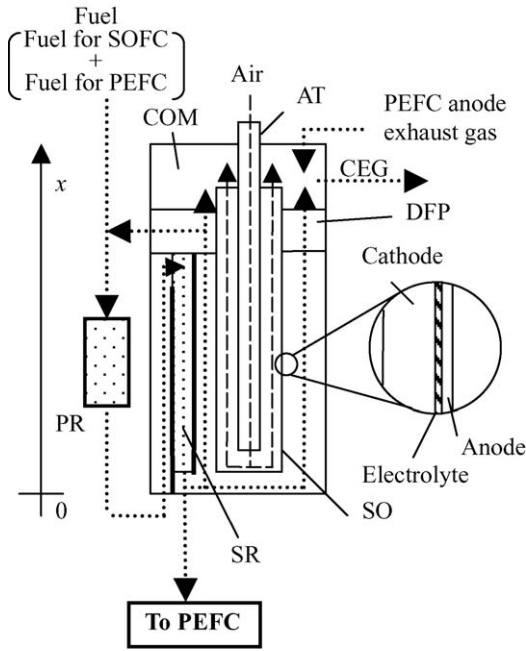
where  $\phi_{\text{SO}}(x)$  is the overpotential of the SOFC,  $J_{\text{SO}}(x)$  the current density of the SOFC, and  $\Gamma$  is the area specified contact resistance between each tubular SOFC [5]. The electromotive force of the SOFC  $E_{\text{SO}}$  is given by:

$$E_{\text{SO}} = -\frac{RT_{\text{SO}}(x)}{4F} \ln \frac{m_{\text{SO-ANO-O}_2}(x)}{m_{\text{SO-CATH-O}_2}(x)}. \quad (7)$$

Part of the SOFC exhaust gas is recycled to the reformer to feed steam. We choose the recycle gas flow rate so that the steam to methane molar fraction ( $S/C$  ratio) at the reformer inlet is 3.0. The remaining anode exhaust gas is burnt with cathode exhaust gas in the combustor. Heat is assumed to be radiated only from the combustor. The air is fed to the alumina tube installed in the tubular SOFC and used for power generation at the cathode. The combustion exhaust gas from the SOFC stack units are gathered and treated as the combustion exhaust gas from the SOFC stack.

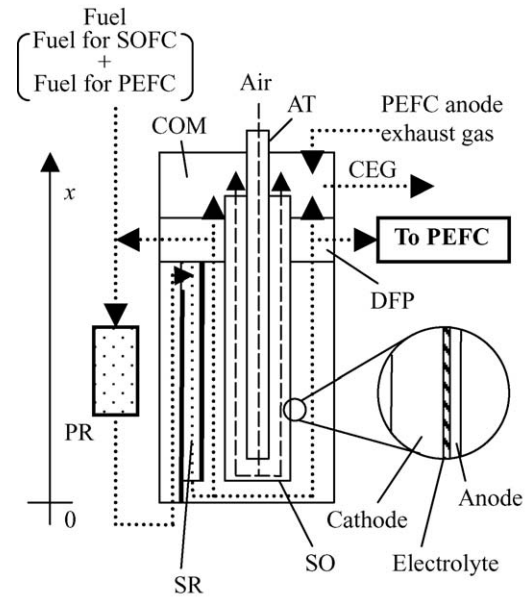
Fig. 6 shows the configuration of the SOFC stack unit for the parallel SOFC–PEFC system. The number of SOFC stack units is also 1152. The stack unit is the same as the one for the simple SOFC system except that the part of the steam reformed fuel is supplied to the PEFC stack and the PEFC anode exhaust gas is fed to the combustor. The PEFC anode exhaust gas is assumed to be distributed to each SOFC unit equally. The cell voltage is calculated based on Eq. (6) so that the average current density of the SOFC stack is kept constant at  $2000 \text{ A m}^{-2}$  though the fuel-and-air-feeding condition is changed in order to use SOFC exhaust heat for the reforming of fuel for PEFC. The flow rate of the reformed fuel fed to the PEFC  $M_{\text{REF-PE}}$  is:

$$M_{\text{REF-PE}} = M_{\text{REF}} - M_{\text{REF-SIMP}}. \quad (8)$$



AT: Alumina tube, CEG: Combustion exhaust gas, COM: Combustor, DFP: Depleted fuel recycling plenum, PR: Pre-reformer, SR: Stack reformer, SO: SOFC

Fig. 6. SOFC stack unit for the parallel SOFC–PEFC system.



AT: Alumina tube, CEG: Combustion exhaust gas, COM: Combustor, DFP: Depleted fuel recycling plenum, PR: Pre-reformer, SR: Stack reformer, SO: SOFC

Fig. 7. SOFC stack unit for the series SOFC–PEFC system.

where  $M_{REF}$  is the flow rate of the reformed fuel and  $M_{REF-SIMP}$  is that of the reformed fuel in the simple SOFC system. That is, the flow rate of reformed gas fed to the tubular SOFC is kept constant in the parallel SOFC–PEFC system, which means that fuel utilization is the same for both the simple and parallel systems.

In the series SOFC–PEFC system, the SOFC stack consists of 1152 SOFC stack units like the one shown in Fig. 7. The SOFC stack unit is the same as one for the simple SOFC system except that the part of SOFC anode exhaust gas is supplied to the PEFC and the PEFC anode exhaust gas is fed to the combustor. As in the parallel SOFC–PEFC system, the PEFC anode exhaust gas is assumed to be distributed to each SOFC unit equally. The cell voltage is calculated based on Eq. (6) so that, again as in the parallel SOFC–PEFC system, the average current density of the SOFC stack is kept constant at  $2000 \text{ A m}^{-2}$ . The flow rate of the SOFC anode exhaust gas fed to the PEFC stack  $M_{SO-ANO-PE}$  is:

$$M_{SO-ANO-PE} = M_{SO-ANO} - M_{SO-ANO-SIMP} \quad (9)$$

where  $M_{SO-ANO}$  is the flow rate of the SOFC anode exhaust gas and  $M_{SO-ANO-SIMP}$  is that of the SOFC anode exhaust gas in the simple SOFC system. The fuel utilization of the SOFC is lower in the series system than in the simple and parallel systems.

The energy balance equations and mass balance equations are same as those used in the previous study [5]. The constants are the same as well [5].

### 3.2. PEFC stacks

The cell areas of the PEFC stacks were varied as the simulation parameter. The cell areas of the PEFC stacks were determined so that the rated net ac outputs would be 25, 50 or 75 kW, based on actual PEFC stack performance [13]. The rated net ac output is defined as the output when the cell voltage is 0.75 V and the current density is  $2000 \text{ A m}^{-2}$  [13]. We refer to the cell voltage of 0.75 V as the designed voltage for the PEFC. The cell areas are listed in Table 1. The cell reaction in the PEFC stack is the oxidation of hydrogen only [14]. The operation temperature of the PEFC is assumed to be 343 K. The partial pressure of steam in the fuel and air fed to the PEFC stack is the saturation vapor pressure. The electromotive force of the PEFC is assumed to be average of those at the PEFC inlet and outlet. The voltage drop in the PEFC stack is assumed to consist of a term that is a linear function of current density and a term that is a logarithm function of current density, where the former corresponds to the ohmic overpotential and the latter to the activation overpotential. That is, from the electromotive force of the PEFC  $E_{PE}$  and the average current density of the PEFC  $J_{PE-AVE}$ , the cell voltage  $V_{PE}$  is calculated so that the average current density of the PEFC stack is  $2000 \text{ A m}^{-2}$  using the equation:

$$V_{PE} = E_{PE} - C_1 J_{PE-AVE} - C_2 \ln \frac{J_{PE-AVE}}{C_3}, \quad (10)$$

where  $C_1$ ,  $C_2$  and  $C_3$  are constants whose values are estimated to be  $2.12 \times 10^{-5}$ ,  $4.07 \times 10^{-2}$  and 1.35, respectively, from the  $I$ – $V$  characteristics of the actual PEFC stack [13]. The  $E_{PE}$  is

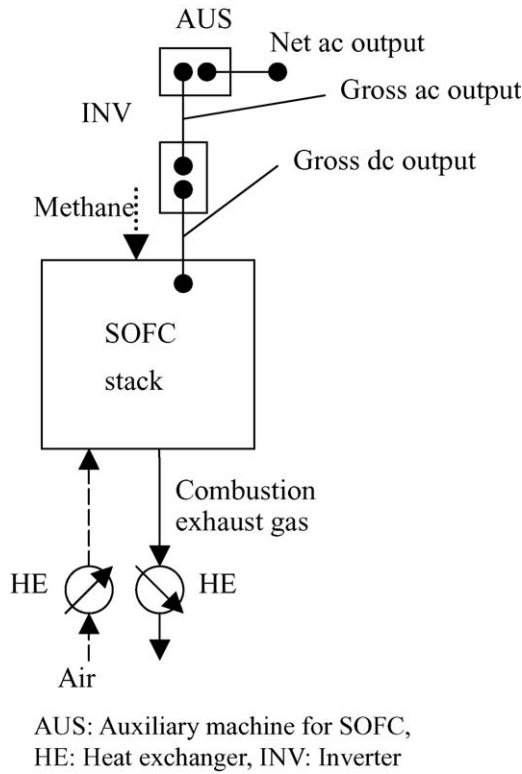


Fig. 8. Configuration of the simple SOFC system.

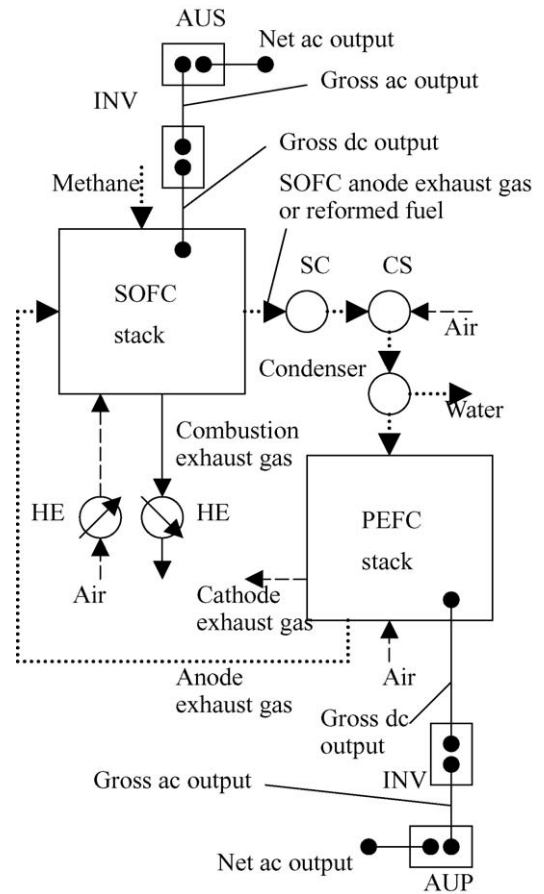


Fig. 9. Configuration of the SOFC–PEFC systems.

calculated by:

$$E_{PE} = -\frac{\Delta G(T_{PE})}{2F} + \frac{RT_{PE}}{4F} \left\{ \ln \frac{m_{PE-H_2-IN} \sqrt{m_{PE-O_2-IN}}}{m_{PE-H_2O-IN}} + \ln \frac{m_{PE-H_2-OUT} \sqrt{m_{PE-O_2-OUT}}}{m_{PE-H_2O-OUT}} \right\}, \quad (11)$$

where  $\Delta G$  is Gibbs free energy change,  $T_{PE}$  the PEFC operation temperature,  $R$  the gas constant. Here,  $m_{PE-H_2-IN}$ ,  $m_{PE-O_2-IN}$  and  $m_{PE-H_2O-IN}$  are the molar fractions of hydrogen, oxygen and steam at the PEFC stack inlet, and  $m_{PE-H_2-OUT}$ ,  $m_{PE-O_2-OUT}$  and  $m_{PE-H_2O-OUT}$  are those molar fractions at the PEFC stack outlet.

### 3.3. Simple SOFC system and SOFC–PEFC systems

The configuration of the simple SOFC system is shown in Fig. 8. The fuel is assumed to be pure methane. The combustion exhaust gas from the SOFC stack is supplied to the heat exchanger and used for raising the air temperature. Gross dc output of the SOFC stack is converted to gross ac output by the inverter. Net ac output is determined by subtracting the power consumed in auxiliary machines from the gross ac output.

The configuration of the parallel and series SOFC–PEFC systems are shown in Fig. 9. The fuels for both cell stacks are also assumed to be pure methane. The reformed fuel is fed to the shift converter in the parallel SOFC–PEFC system, whereas the SOFC anode exhaust gas is fed to it in the series SOFC–PEFC system. The flow rate of methane for the PEFC is determined so that the fuel utilization of the PEFC stack is 70%, which is the fuel utilization in an actual simple PEFC system [13]. The

fuel utilization of the PEFC stack  $U_{PE-FUEL}$  is assumed to be the ratio of the hydrogen used for power generation to that fed to the PEFC. That is,  $U_{PE-FUEL}$  is defined as:

$$U_{PE-FUEL} = 1 - \frac{J_{PE-TOT}}{2FM_{PE-H_2}}, \quad (12)$$

where  $J_{PE-TOT}$  is total current of the PEFC stack,  $M_{PE-H_2}$  the flow rate of hydrogen in the gas fed to the PEFC stack, and  $F$  is the Faradays constant. Ninety-nine percent of the carbon monoxide in the gas fed to the shift converter is converted to carbon dioxide according to the shift reaction in the shift converter. The fuel passes through the shift converter and is fed to the CO selective oxidizer. Carbon monoxide in the gas fed to the CO selective oxidizer is completely oxidized to carbon dioxide. The reaction in the CO selective oxidizer is the oxidation of carbon monoxide only. The fuel from the CO selective oxidizer is supplied to the condenser to decrease the fuel temperature and to remove excess water. The fuel from the condenser is supplied to the PEFC stack. The SOFC stack and the PEFC stack have an inverter and auxiliary machines. Like the net ac output of the SOFC stack, that of the PEFC stack is determined by subtracting the power consumed in auxiliary machines from the gross ac output, which

is converted from gross dc output by using the inverter. The net ac output and electrical efficiency at net ac are calculated by the same equations as in our previous study [5].

## 4. Results and discussion

### 4.1. Comparison of simulation with experimental results

We compared the simulation result for the simple SOFC system with the experimental result for an actual simple SOFC system [2,15]. The comparison is summarized in Table 2. The simulation result agreed with the experimental result, which indicates that our simulation can estimate the electrical efficiency, output, and temperature distribution in the simple SOFC system. The simulation result and the experimental result for the  $I$ – $V$  characteristic of the PEFC stack are shown in Fig. 10. The simulation result agreed with the experimental result. Our simulation can estimate the performance of the PEFC stack. Consequently, we concluded that our simulation could estimate the performance of the SOFC–PEFC systems.

### 4.2. Simulation results for the parallel SOFC–PEFC system

The simulation results for the parallel SOFC–PEFC system are summarized in Table 3. The reforming heat  $Q_{REF}$  increases with increasing rated output, since the SOFC exhaust heat is used for the reforming of fuel for PEFC increases. The SOFC voltage  $V_{SO}$  in the parallel SOFC–PEFC system is as same as that in the simple SOFC system when the rated net ac output of the PEFC stack is 25 or 50 kW. On the contrary, the  $V_{SO}$  in

Table 3  
Simulation results for the parallel SOFC–PEFC system

	$Q_{REF}$ (kW)	$V_{SO}$ (V)	$W_{SO-ac}$ (kW)	$V_{PE}$ (V)	$W_{PE-ac}$ (kW)	$\eta_{ac}$ (%)	$W_{SYS-ac}$ (kW)
Simple SOFC system	47	0.65	114			47	114
25-kW-class PEFC stack	63	0.65	115	0.75	25	49	140
50-kW-class PEFC stack	77	0.65	115	0.75	50	50	165
75-kW-class PEFC stack	90	0.64	116	0.75	75	51	191

the parallel SOFC–PEFC system is slightly lower than that in the simple SOFC system when the rated net ac output of the PEFC stack is 75 kW. That is, the  $V_{SO}$  slightly decreases with increasing  $Q_{REF}$ . This is because the temperature gradient of the solid oxide electrolyte increases with increasing  $Q_{REF}$  and because the molar fraction of the oxygen at the cathode side of the tubular SOFC decreases with increasing  $Q_{REF}$ .

The temperature profile of the solid oxide electrolyte in the parallel SOFC–PEFC system is shown in Fig. 11. We refer to the region where  $x/L$  is smaller than 0.5 as the bottom side and refer to that where  $x/L$  is larger than 0.5 as the top side. The temperature of solid oxide electrolyte  $T_{SO}$  decreases with increasing  $Q_{REF}$  at the top side. This is because the steam reforming reaction mainly occurs there, since the reaction rate of the steam reforming decreases as the reaction proceeds [5,16]. Note that  $x/L$  of the steam reformer inlet is 1.0. On the contrary, the  $T_{SO}$  increases with increasing  $Q_{REF}$  at the bottom side, where the steam reforming reaction does not occur. This is because the SOFC exhaust heat is mainly absorbed in the air flow at the bottom side, and the SOFC exhaust heat discharged with the air flow  $Q_{AIR}$  decreases with increasing  $Q_{REF}$  as shown in Fig. 4. The decrement of the  $T_{SO}$  for  $Q_{REF}$  at the top side is larger, which means the temperature gradient increases with increasing  $Q_{REF}$ . The larger temperature gradient leads to lower average temperature and cell performance since the maximum  $T_{SO}$  is kept constant at 1273 K.

The molar fraction of the oxygen at the cathode side of tubular SOFC decreases with increasing reforming heat  $Q_{REF}$ , since

Table 2  
Comparison of experimental and simulation results for the simple SOFC system

	Experimental [12]	Simulation
Electrical efficiency at net ac (%)	46	47
Net ac output (kW)	109	114
Cell voltage (V)	0.66	0.65
Recycling gas temperature (K)	1173	1083
Pre-reformed gas temperature (K)	823	772
Average cell temperature (K)	1203	1202
Maximum cell temperature (K)	1273	1273
Minimum cell temperature (K)	1083	1114

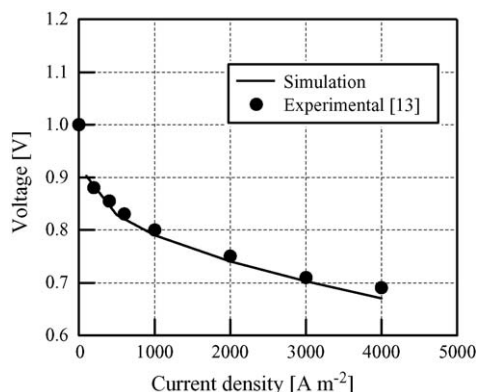


Fig. 10. Comparison of experimental and simulation results for the PEFC stack.

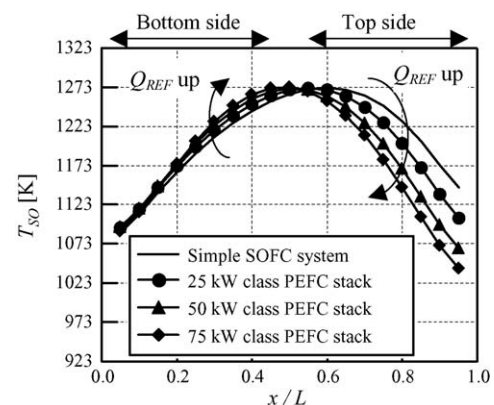


Fig. 11. Temperature profile of the solid oxide electrolyte in the simple SOFC and parallel SOFC–PEFC systems.

Table 4

Averaged molar fraction of each gas component at the cathode and anode side of the tubular SOFC in the parallel SOFC–PEFC system

	O <sub>2</sub>	H <sub>2</sub>	H <sub>2</sub> O	CO	CO <sub>2</sub>
Simple SOFC system	0.18	0.25	0.42	0.14	0.19
25-kW-class PEFC stack	0.18	0.25	0.42	0.14	0.19
50-kW-class PEFC stack	0.16	0.25	0.42	0.14	0.19
75-kW-class PEFC stack	0.15	0.25	0.42	0.14	0.19

the air fed to the tubular SOFC is decreased to increase the  $Q_{REF}$  as shown in Fig. 4. The electromotive force of the SOFC  $E_{SO}$  is lower when the molar fraction of the oxygen at the cathode side of the tubular SOFC is lower (see Eq. (7)). The lower electromotive force leads to lower cell voltage when the current density is constant. The averaged molar fractions of oxygen at the cathode side of the tubular SOFC are listed in Table 4, which also lists the averaged molar fraction of each gas component at the anode side. The averaged molar fraction of each gas component at the anode side of tubular SOFC is same for all systems listed in Table 4. This is because the flow rate of the reformed fuel fed to the tubular SOFC in the parallel SOFC–PEFC system is the same as that in the simple SOFC system regardless of the rated output of the PEFC stack (see Eq. (8)). Note that methane also exists at the anode side of the tubular SOFC, though it is not listed in Table 4. The molar fraction of methane is on the order of  $10^{-5}$ , so its effect is negligible.

As shown in Table 3, the net ac output of the SOFC stack  $W_{SO-ac}$  slightly increases with increasing  $Q_{REF}$ , although the  $V_{SO}$  in the parallel SOFC–PEFC system slightly decreases with increasing  $Q_{REF}$ . The reason for this is as follows. The gross dc output of the SOFC stack decreases with increasing  $Q_{REF}$  since  $V_{SO}$  decreases. However, the auxiliary power consumption decreases with increasing  $Q_{REF}$ , since the power consumption of the air blower, which is dominant power consumption, decreases with increasing  $Q_{REF}$  (see Fig. 4). The decrement of the auxiliary power consumption exceeds the decrement of the gross dc output. The  $W_{SO-ac}$ , the gross ac output minus auxiliary power consumption, therefore increases with increasing  $Q_{REF}$ .

The PEFC voltage  $V_{PE}$  is constant at 0.75 V, which is same as the designed cell voltage for the PEFC. This means that the molar fraction of hydrogen in the reformed gas fed to the PEFC stack is high enough to operate the PEFC stack at the designed point. The molar fraction of each gas component in the reformed gas fed to the PEFC stack in the parallel SOFC–PEFC system is listed in Table 5. The net ac outputs of the PEFC stacks are the rated output in all parallel SOFC–PEFC systems listed in Table 2, since the PEFC stack is operated at the designed cell voltage of 0.75 V.

Table 5

Molar fraction of each gas component in the gas fed to the PEFC stack in the parallel SOFC–PEFC system

	H <sub>2</sub>	H <sub>2</sub> O	CO <sub>2</sub>
25-kW-class PEFC stack	0.44	0.31	0.25
50-kW-class PEFC stack	0.44	0.31	0.25
75-kW-class PEFC stack	0.44	0.31	0.25

Table 6

Simulation results for the series SOFC–PEFC system

	$Q_{REF}$ (kW)	$V_{SO}$ (V)	$W_{SO-ac}$ (kW)	$V_{PE}$ (V)	$W_{PE-ac}$ (kW)	$\eta_{ac}$ (%)	$W_{SYS-ac}$ (kW)
Simple SOFC system	47	0.65	114			47	114
25-kW-class PEFC stack	67	0.69	122	0.74	25	50	147
50-kW-class PEFC stack	77	0.70	124	0.74	49	54	173

The electrical efficiency  $\eta_{ac}$  increases with increasing  $Q_{REF}$ , since the utilization of SOFC exhaust heat contributes to the electrical efficiency [5,6]. The  $\eta_{ac}$ 's are 49, 50 and 51% when the rated output of the PEFC stack is 25, 50 and 75 kW, respectively. Note, that there is a limit to how far the rated output of the PEFC stack can be increased. This is because we cannot supply the sufficient steam required for the steam reforming reaction by recycling the SOFC anode exhaust gas when the rated PEFC output exceeds a certain limit. When the rated PEFC output is 75 kW for the 100-kW-class SOFC stack, almost all SOFC anode exhaust gas is recycled to the reformer to feed the steam. This means a PEFC stack that has rated output larger than 75 kW cannot be operated at the designed point in the parallel SOFC–PEFC system.

Net ac outputs of the parallel SOFC–PEFC system are 140, 165 and 191 kW when the rated output of the PEFC stack is 25, 50 and 75 kW, respectively.

#### 4.3. Simulation results for series SOFC–PEFC system

The simulation results for the series SOFC–PEFC system are summarized in Table 6. There is also some limit on the PEFC output in the series SOFC–PEFC system. The limit is lower for the series SOFC–PEFC system than for the parallel SOFC–PEFC system. This is because the molar fraction of steam in the SOFC anode exhaust gas is lower in the series SOFC–PEFC system, since the fuel utilization of the SOFC in the series SOFC–PEFC system is lower than in the parallel SOFC–PEFC system as mentioned above. We have to recycle much more SOFC exhaust gas to feed sufficient steam for the same amount of fuel for the PEFC in the series SOFC–PEFC system. Therefore, the maximum rated output of the PEFC stack that can be operated in the series SOFC–PEFC system is lower.

The reforming heat  $Q_{REF}$  increases with increasing rated output also in the series SOFC–PEFC system. The amount of  $Q_{REF}$  for the same rated PEFC stack output is almost the same in the parallel and series SOFC–PEFC systems. This is because the amount of fuel for the PEFC is almost the same when the rated output of the PEFC stacks is the same. The cell voltage of the tubular SOFC  $V_{SO}$  in the series SOFC–PEFC system increases with increasing  $Q_{REF}$ . This tendency is quite different from that in the parallel SOFC–PEFC system. In what follows, we will explain the reason for this using the temperature profiles of the solid oxide electrolyte and the molar fraction of each gas component.

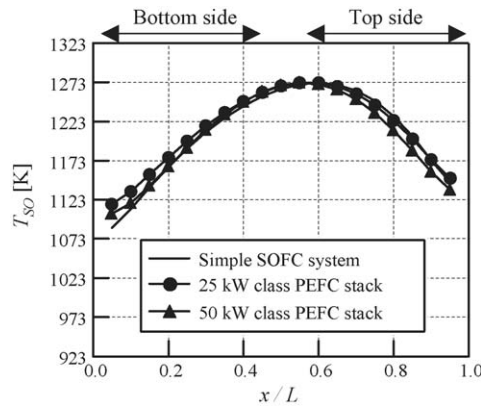
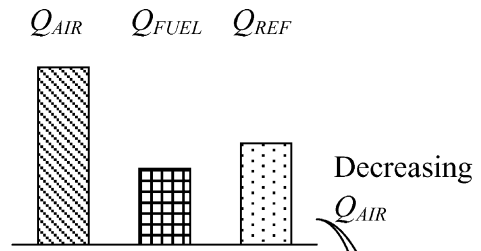


Fig. 12. Temperature profile of the solid oxide electrolyte in the simple SOFC and series SOFC–PEFC systems.

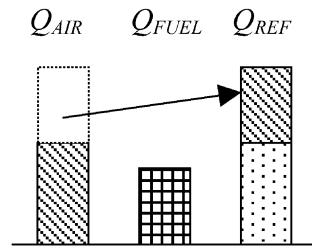
The temperature profiles of the solid oxide electrolyte in the series SOFC–PEFC system are almost the same as those in the simple SOFC system independent of the rated output of the PEFC stack as shown in Fig. 12. Although the temperature profile of the solid oxide electrolyte in the series SOFC–PEFC system slightly changes as the  $Q_{REF}$  changes like in the parallel SOFC–PEFC system, the magnitude of the temperature shift is certainly smaller in the series SOFC–PEFC system. This difference is attributed to the difference in the SOFC exhaust heat utilization mechanism between the parallel and series SOFC–PEFC systems. The whole decrement of  $Q_{AIR}$  is converted to  $Q_{REF}$  in the parallel SOFC–PEFC system, whereas part of  $Q_{AIR}$  is converted to  $Q_{REF}$  in the series SOFC–PEFC system, as shown in Fig. 13. The rest of  $Q_{AIR}$  is converted to  $Q_{FUEL}$  in the series SOFC–PEFC system, since the all reformed fuel is fed to the tubular SOFC as shown in Fig. 3. Here,  $Q_{FUEL}$  is the SOFC exhaust heat absorbed into the fuel flow. The temperature gradient in the series SOFC–PEFC system is smaller, because the amount of  $Q_{FUEL}$  is larger and because the fuel flow takes heat both from the top and bottom side. The temperature shift is not a dominant factor in the SOFC voltage.

The averaged molar fraction of each gas component at the cathode and anode side of the tubular SOFC in the series SOFC–PEFC system is listed in Table 7. The averaged molar fraction of the oxygen at the cathode side of tubular SOFC decreases with increasing reforming heat  $Q_{REF}$ , also in the series SOFC–PEFC system. The averaged molar fraction of oxygen for the same rated output of the PEFC stack is smaller in the series SOFC–PEFC system than in the parallel SOFC–PEFC system (compare Tables 4 and 7). This is because the whole decrement of  $Q_{AIR}$  is converted to  $Q_{REF}$  in the parallel SOFC–PEFC system, whereas part of  $Q_{AIR}$  is converted to  $Q_{REF}$  in the series

Simple SOFC system



Parallel SOFC-PEFC system



Series SOFC-PEFC system

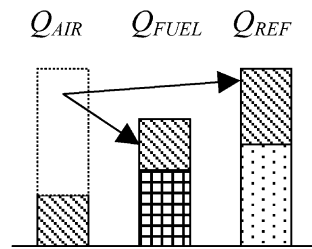


Fig. 13. Difference in the SOFC exhaust heat utilization mechanism between parallel and series SOFC–PEFC systems.

SOFC–PEFC system, as mentioned above by using Fig. 13. So, the decrement of air fed to the tubular SOFC has to be larger in the series SOFC–PEFC system when  $Q_{REF}$  in both systems is the same. In contrast to the parallel SOFC–PEFC system, the averaged molar fractions of hydrogen and carbon monoxide at the anode side of tubular SOFC increase with increasing  $Q_{REF}$  and those of steam and carbon dioxide decrease with increasing  $Q_{REF}$  in the series SOFC–PEFC system. This is because the fuel utilization of SOFC decreases with increasing  $Q_{REF}$ , since all reformed fuel is fed to the tubular SOFC in the series SOFC–PEFC system and the average current density of the tubular SOFC is kept constant. In the series SOFC–PEFC system, the change of molar fraction with increasing  $Q_{REF}$  at the cathode side of the tubular SOFC has a negative contribution to cell voltage, though those at the anode side have a positive contribution. The latter effect exceeds the former. That is, the  $V_{SO}$  in the series SOFC–PEFC system increases with increasing  $Q_{REF}$ .

The net ac output of the SOFC stack  $W_{SO-ac}$  in the series SOFC–PEFC system increases with increasing  $Q_{REF}$  as shown in Table 6. This is because the cell voltage of the tubular SOFC  $V_{SO}$  in the series SOFC–PEFC system increases with increasing

Table 7  
Averaged molar fraction of each gas component at cathode and anode side of the tubular SOFC in the series SOFC–PEFC system

	O <sub>2</sub>	H <sub>2</sub>	H <sub>2</sub> O	CO	CO <sub>2</sub>
Simple SOFC system	0.18	0.25	0.42	0.14	0.19
25-kW-class PEFC stack	0.17	0.34	0.32	0.19	0.15
50-kW-class PEFC stack	0.14	0.38	0.29	0.21	0.12

Table 8

Molar fraction of each gas component in the gas fed to the PEFC stack in the series SOFC–PEFC system

	H <sub>2</sub>	H <sub>2</sub> O	CO <sub>2</sub>
25-kW-class PEFC stack	0.38	0.31	0.31
50-kW-class PEFC stack	0.41	0.31	0.28

$Q_{REF}$  as mentioned above, and because the auxiliary power consumption decreases with increasing  $Q_{REF}$ .

The cell voltage of the PEFC  $V_{PE}$  in the series SOFC–PEFC system is 0.74 V for both the 25 and 50-kW-class PEFC stack. This voltage is slightly lower than the designed voltage for the PEFC, which is 0.75 V (Section 3.2). This means that molar fraction of hydrogen in the SOFC anode exhaust gas fed to the PEFC stack is not high enough to operate the PEFC stack at the designed point. The molar fraction of the each gas component in the SOFC anode exhaust gas fed to the PEFC stack in the series SOFC–PEFC system is listed in Table 8. In the series SOFC–PEFC system, the molar fraction of hydrogen is higher when the rated output of the PEFC stack is 50 kW than when it is 25 kW. This is because the molar fraction of hydrogen in the SOFC anode exhaust gas is higher when the rated output of the PEFC stack is 50 kW. However, the molar fraction of hydrogen in the SOFC anode exhaust gas in the series SOFC–PEFC system is lower than that in the reformed gas in the parallel SOFC–PEFC system, even though the rated output of the PEFC stack is 50 kW (compare Tables 5 and 8). The net ac outputs of the PEFC stacks are 25 and 49 kW in the series SOFC–PEFC system when the rated output of the PEFC stack is 25 and 50 kW, respectively. That is, the 25-kW-class PEFC stack is operated at the designed output in the series SOFC–PEFC system, though the  $V_{PE}$  is slightly lower than the designed value. However, the net ac output of the 50-kW-class PEFC stack is slightly lower than the rated net ac output since the  $V_{PE}$  is slightly lower than the designed value.

The electrical efficiency  $\eta_{ac}$  increases with increasing  $Q_{REF}$  also in the series SOFC–PEFC system. The  $\eta_{ac}$  is 50 and 54% when the rated output of the PEFC stack is 25 and 50 kW, respectively. The  $\eta_{ac}$  for the same rated output of the PEFC stack is higher in the series SOFC–PEFC system than in the parallel SOFC–PEFC system (compare Tables 3 and 6). This is because the cell voltage of the SOFC is certainly higher in the series SOFC–PEFC system, though the cell voltage of the PEFC is slightly lower than in the parallel SOFC–PEFC system. Here, we will explain the reason. The  $V_{SO}$  is higher and the  $V_{PE}$  lower in the series SOFC–PEFC system (compare Tables 3 and 6). The differences in the cell voltages mainly depend on the differences in the molar fractions of the gas components, which determine the electromotive force by the Nernst equation (Eqs. (7) and (11)). It is clear that the effect of the molar fractions on electromotive force becomes pronounced when the operation temperature is high. Thus,  $V_{SO}$  is clearly higher in the series SOFC–PEFC system, though the  $V_{PE}$  is slightly higher in the parallel SOFC–PEFC system because of the low operation temperature. Therefore, the difference in the molar fractions of the gas components in the gas fed to the SOFC causes the clear dif-

ference in  $V_{SO}$ , though that in the gas fed to the PEFC cause little difference in  $V_{PE}$ .

Net ac outputs of the series SOFC–PEFC system  $W_{SYS-ac}$  are 147 and 173 kW when the rated outputs of the PEFC stack is 25 and 50 kW, respectively. The  $W_{SYS-ac}$  for the same rated output of the PEFC stack is larger in the series SOFC–PEFC system than in the parallel SOFC–PEFC system (compare Tables 3 and 6). This is because the net ac output of the SOFC stack  $W_{SO-ac}$  for the same rated output of the PEFC stack is larger in the series SOFC–PEFC system. However, we have to emphasize that the 75-kW-class PEFC stack can be operated in the parallel SOFC–PEFC system and the net ac output of the parallel SOFC–PEFC system with the 75-kW-class PEFC stack is higher than that of the series SOFC–PEFC system with the 50-kW-class PEFC stack.

## 5. Conclusion

We quantitatively evaluate performance of a series-fuel-feeding-type SOFC–PEFC system (series SOFC–PEFC system) and a parallel-fuel-feeding-type SOFC–PEFC system (parallel SOFC–PEFC system). The main results are as follows. Larger PEFC output can be obtained in the parallel SOFC–PEFC system when the same SOFC stack is used, which means that the parallel SOFC–PEFC system is appropriate for larger output. On the contrary, the series SOFC–PEFC system can provide higher electrical efficiency than the parallel SOFC–PEFC system when the same SOFC stack and the same PEFC stack are used.

## References

- [1] J. Larminie, A. Dicks, Fuel Cell Systems Explained, John Wiley & Sons, 2000, pp. 123–134.
- [2] R.A. George, J. Power Sources 86 (2000) 134–139.
- [3] S.E. Veyo, W.L. Lundberg, in: Proceeding of the international Gas Turbine & Aeroengine Congress & Exhibition, Paper 99-GT-550, 1999.
- [4] S.E. Veyo, L.A. Shockling, J.T. Dedere, J.E. Gillett, W.L. Lundberg, in: Proceeding of the international Gas Turbine & Aeroengine Congress & Exhibition, Paper 2000-GT-550, 2000.
- [5] M. Yokoo, T. Take, J. Power Sources 137 (2004) 206–215.
- [6] M. Yokoo, K. Watanabe, M. Arakawa, Y. Yamazaki, J. Power Sources 146 (2005) 315–318.
- [7] H.E. Vollmar, C.U. Maier, C. Nolscher, T. Merklein, M. Poppinger, J. Power Sources 86 (2000) 90–97.
- [8] A.L. Dicks, R.G. Fellows, C.M. Mescal, C. Seymour, J. Power Sources 86 (2000) 501–506.
- [9] W.L. Lundberg, Proceedings of the Symposium on Fuel Cells, 1989, pp. 118–129.
- [10] T. Iwanari, N. Miyauchi, K. Ito, K. Onda, Y. Sasaki, S. Nagata, Trans. Jpn. Soc. Mechanical Eng., Ser. B 68 (673) (2002) 214–220 (in Japanese).
- [11] S. Nagata, Y. Kasuga, Y. Ono, Y. Kaga, H. Sato, Trans. Inst. Electrical Eng. Jpn. 107 (B-3) (1982) 147–154 (in Japanese).
- [12] S.C. Singhal, The Electrochemical Society Proceedings, Solid Oxide Fuel Cell V, vol. 97-18, 1997, pp. 37–50.
- [13] T. Yateke, A. Sonai, S. Matsuda, A. Kano, Proceedings of Fuel Cell Symposium, 2001, pp. 76–83 (in Japanese).
- [14] L.J.M.J. Blomen, M.N. Mugerwa, Fuel Cell Systems, Plenum Press, 1993, pp. 493–495.
- [15] R.A. George, A.C. Casanova, S.E. Veyo, Fuel Cell Seminar Abstracts, 2002, pp. 977–979.
- [16] T. Take, T. Yamashita, M. Tomura, J. Chem. Eng. Jpn. 33 (2000) 67–77.